Wear 266 (2009) 934–944

Contents lists available at ScienceDirect

Wear

journal homepage: www.elsevier.com/locate/wear

Short-pitch rail corrugation: A possible resonance-free regime as a step forward to explain the "enigma"?

L. Afferrante, M. Ciavarella*

CEMEC-PoliBA - Via Re David 200, Politecnico di Bari, 70124 Bari, Italy

ARTICLE INFO

Article history:
Received 10 April 2008
Received in revised form 17 November 2008
Accepted 2 December 2008
Available online 7 December 2008

Keywords:
Short pitch corrugation
Rolling contact
Wear
Friction instabilities

ABSTRACT

Rail corrugation has been noticed at least for 100 years, but (particularly short pitch one in the range 20–80 mm) has been considered an enigma because measured corrugation wavelength did not relate well with wear-instability models. The apparently large number of governing parameters has resulted in many independent efforts to generate models, which do not entirely correspond to the collected experimental evidence, and therefore there is still some uncertainty over the possible critical factors dominating the phenomenon.

We show in the paper that there is a simple possible mechanism of corrugation in longitudinal direction, apparently not noticed before in the literature by other authors, which does not necessarily correspond to a resonance in the system, not even the pinned–pinned resonance associated with the effect of discrete supports, but may depend on geometrical and loading conditions (normal load, creepage ratio, shape of the contact area, etc.), in general overall agreement with experiments.

Additionally, some approximate calculations including discrete supports, using a typical concrete sleepers vertical receptance of BR use, show no evidence of corrugation mechanism at the pinned–pinned resonance, at least in the longitudinal direction. A full comparison between lateral and longitudinal mechanisms would depend on the particular value of the lateral creepage vs. longitudinal creepage, system-specific. The present "resonance-free" mechanism is a possible alternative for the data which fall outside the pinned–pinned resonance range.

1. Introduction

Corrugation caused by the action of the railways wheels is a phenomenon observed throughout railways history (i.e. at least in the last 100 years) but not fully understood [1] particularly for short-pitch rail corrugation ("roaring rails") in the range of 20–80 mm wavelength.

Most available data seem to show a non-linearly increasing wavelength with speed, i.e. an almost fixed-wavelength and not fixed-frequency feature if one searches a single mechanism (as probably the earlier authors were doing) (see Fig. 1 adapted from Fig. 1 of Bhaskar et al. [2], with quite a lot of data in BR reports in 1911, David Harrison's Cambridge Ph.D. thesis [3] and the Vancouver SkyTrain data). However, if one accepts many possible regimes at work, one not necessarily sees the "non-linearity".

Instead, most models generally obtain a resonance on the system, the most obvious being the vertical direction ones, like in the early Hertz spring "contact resonance" mechanism of Carson and Johnson [4] and Johnson and Gray [5], or the P2 or "loaded track" resonance, both of which have frequency of less than about 100 Hz, inducing corrugation wavelengths several centimeters long for the typical train speeds found in these resonances.

In the range of frequency of short-pitch corrugation, the normal force has its peak near the crest of the corrugation, and hence a mechanism of plastic impacts cannot be active, as confirmed by evidence suggesting plastic deformation (and sometimes martensitic transformations) occurs on the peaks but not on the troughs [6], and instead evidence of slip and wear. However, Frederick also reported open hearth rail steel is much less prone to corrugate than Acid Bessemer, and in general high plastic deformation resistant materials show corrugation quickly, although the increase of wear resistance slows the rate of formation. Therefore, a more complete model probably should consider *competing* plastic and wear mechanisms.

The first simple model involving a differential wear mechanism with longitudinal creepage like in braking or acceleration, was suggested by Grassie and Johnson [7], but instead of explaining corrugation, seemed to act as *suppressing* corrugation. By now, after about 15 years of research in Cambridge and at BR, the puzzle of rail corrugation started to be spoken of as an "enigma". Ciavarella and Barber [8] recently suggested that this conclusion comes from erroneously assuming constant longitudinal creepage and when the

* Corresponding author. Tel.: +39 080 5962811; fax: +39 080 5962777.
E-mail address: mciava@poliba.it (M. Ciavarella).

0043-1648/$ – see front matter © 2008 Elsevier B.V. All rights reserved.
doi:10.1016/j.wear.2008.12.003

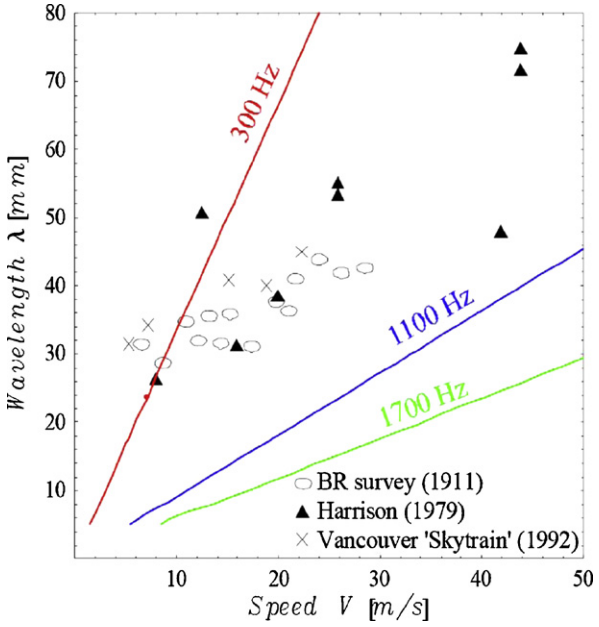

Fig. 1. Variation of corrugation wavelength with speed (data from Bhaskar et al. [2], Fig. 1). Superposed are 3 lines which refer to the most commonly frequencies associated to models of short pitch corrugation, clearly remote from most data points.

inertia of the wheel and the rotational dynamics of the system are considered, a much better qualitative agreement with experimental evidence is immediately found.

Later, BR introduced quite a few innovations in the Frederick model [6], with discrete supports, a sort of perturbation approach using complex transfer functions, and a detailed treatment of the receptances in both lateral longitudinal and vertical direction, including also the mass of the wheel (as a concentrated mass) in the analysis, hence a model not only satisfying the requirements but much richer than Ciavarella and Barber [8]. Frederick did find a few possible regimes of corrugation, but still he made a few assumptions and an approximate treatment for the discrete support effect. He reached the conclusion that the dominant mechanism would be *lateral corrugation* at the pinned–pinned resonance at about 800–1100 Hz in most railways systems, in which the rail vibrates almost as if it were a beam pinned at sleepers, which is strictly due to the effect of including the discrete nature of supports. Later, many models assume this is a likely mechanism for corrugation, and lately has actually been associated to a firm and definitive source of short-pitch corrugation in a recent review by Grassie [9]:- *. . .it is now clear that the wavelength-fixing mechanism for this type of corrugation, on which the author believed it prudent to hold an "agnostic" view in 1993 [7], is indeed the so-called "pinned–pinned" resonance, in which the rail vibrates as if pinned at the sleepers. This is demonstrated convincingly by the linear modelling of Hempelmann from TUB. . .. The frequency of this mode is typically about 800 Hz in the UK, for a sleeper spacing of 0.75 m and 56 kg/m rail, whereas in much of continental Europe it is more commonly about 1200 Hz because of the closer sleeper spacing (0.6 m) and heavier rail section (60 kg/m) [10]. The search for a mechanism that would give a constant wavelength, which had been central to the joint British Rail Research and Cambridge University research project in the 1970s and 1980s, is evidently a chimera that had emerged because types of corrugation that arise from different mechanisms were then believed to have had the same cause*.

However, we think that it is still prudent to hold an "agnostic view" even today, since the original data collected by British Rail Research and Cambridge University, which are probably still the most reliable around, are still *not* explained in terms of pinned–pinned resonance, as it is clear from Fig. 1. Therefore, while we agree that there is not a single mechanism, we disagree that pinned–pinned resonance is so clearly uniquely responsible for short pitch corrugation. Also, short-pitch corrugation appeared very strongly on Vancouver SkyTrain which has not a typical discrete support, and indeed did not change when the spacing of support changed (see Bhaskar et al. [2]).

It may be possible that the influence of the pinned–pinned resonance has been overestimated because:

(1) *models with continuum support* (Grassie and Johnson [7], Bhaskar et al. [2]) have partly failed in quantitative prediction of wavelength because of the erroneous tangential dynamics assumptions, in particular, constant creepage. When the wheel inertia and the transient contact mechanics effects are considered, like shown in a recent model [8] using a continuum description of the rail (hence neglecting pinned–pinned resonance), the results seem to show a few possible regimes where many wavelengths are unstable at low speed, and an apparent regime of highest growth just above 400 Hz, not too remote from the experimental evidence. At the other end of the spectrum, some models [10,11] assume constant tangential load, and this is seen to show corrugation growth, perhaps exaggerated. In this category falls also the model of Xie and Iwnicki [12] who however seems to find that all initial sinusoidal roughness of wavelengths between 20 and 100 mm are levelled out if one considers the full models with non-steady effects included, whereas growth is only possible with a simplified "steady" model. Somehow in contrast with this, Knothe and Groß-Thebing [13] suggest critical importance of the "filtering" effect of non-steady contact mechanics, particularly in explaining why corrugation smaller than 20 mm is not found.

(2) *models with discrete supports* (Frederick [6], Hempelmann and Knothe [14], Hempelmann [15]), in the attempt to introduce their effect, tend to exaggerate the role of the pinned–pinned resonance. In fact, they generally use local eigenvalue analysis, which means that they assume a steady state is reached like if the local receptance were valid for an infinite length. This may exaggerate the amplification of normal load (or of lateral loads, or both) above sleepers by a significant factor (for example, from Grassie et al. [1], we estimated the error can be easily a factor 2 if not larger[1]). In particular, Hempelmann and Knothe [14], Hempelmann [15], *only* looked at the lateral direction perhaps because of the indication from [6] that in longitudinal direction the phase appears not appropriate for corrugation, despite Frederick himself in a discussion of Hempelmann and Knothe's paper, question this simplification as "longitudinal creepage tends to be much higher than lateral". More recent models with discrete support include *parametric resonance* (Wu and Thompson [16], Sheng et al. [17], Wu and Thompson [18], which deal with noise rather than corrugation). The effects are very difficult even to describe and to study, they depend on stiffness of the pad, a peak with the "local" calculation becomes distinctly mid-sleepers at frequencies actually higher than the pinned–pinned resonance (1200–1400 Hz) rather than that at above sleepers. The "local" approach should be correct when the ratio wavelength of corrugation over sleepers distance is small. Hence,

[1] In Grassie et al. [19], calculated dynamic loads for a continuous model (see his Fig. 3) without discrete supports are compared with measurements by load measuring wheel (see his Fig. 12). The highest load is at about 1000 Hz, about 2.8 times higher than at 600 Hz. We estimated the same increase to be a factor 5 with a "local" use of receptances as in the Frederick or Hempelmann "moving perturbation" models, for a BR track with the standard "Grassie" 280 MN/m stiff pad.

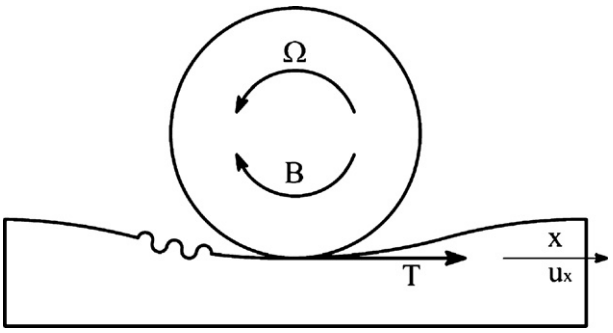

Fig. 2. Coordinate system for the rotating wheel.

the very short wavelengths should be correctly modelled with the local approach. We shall use in effect in our last paragraph a local model to deal with discrete support effects, limited to longitudinal direction.

So with this sort of background, we decided to look at the simplest possible model, given we are not in a position to easily check results in the literature with often sophisticated numerical simulations. To us, a lot more validation is needed for even the simplest of these numerical models, and our own efforts to produce clean and closed form solutions is also along the lines of extending the possibilities to check these models. With respect to the previous contributions, here we improve the treatment from Ciavarella and Barber [8] as they assumed a simple full stick Winkler contact mechanics. Far from having the ambition to give a definitive and final word on this complicated problem, we shall simply elucidate the effect of contact geometry in the likely short-pitch corrugation regime, removing the Winkler approximation, and using a continuous analytical solution approximately valid for 3D elliptical contact areas, and in partial slip. To simplify the discussion, we shall use an extremely simplified vertical receptance model, but valid in the frequency range greater than 500 Hz, of course under the assumption of neglecting pinned–pinned resonance due to discrete supports. In doing the approximate 3D treatment, we differ from a previous attempt by Bhaskar et al. [2] who used a model validated only for variations of tangential load.

2. The model

The model under investigation is initially that proposed in Barber et al. [20](see Fig. 2). For a wheel rotating with radius R over a corrugated rail translating with velocity V, and concentrating all the elastic deformation in the wheel (we shall use an equivalent modulus for the wheel and treat the rail as rigid, in the tangential direction), we can define a slip velocity in terms of the tangential displacements of the contacting points u_x. The condition of zero slip (assuming the coefficient of friction is sufficiently high to prevent slip occurring anywhere), gives a partial differential equation for u_x. Barber et al. [20] have shown how to find a small perturbation solution, i.e. assuming that $\Omega(t)$ is a known function of the form

$$\Omega(t) = \Omega_0 + \Omega_1 \exp(\iota\omega t), \tag{1}$$

where ω is the circular frequency and every other quantity has a steady state and an oscillating component. For example, the normal and tangential forces P, Q have the sinusoidal form

$$P(t) = P_0 + P_1 \exp(\iota\omega t); \quad 1Q(t) = Q_0 + Q_1 \exp(\iota\omega t), \tag{2}$$

where P_0, P_1, Q_0, Q_1 are constants and $P_1 \ll P_0$, $Q_1 \ll Q_0$. Also, the instantaneous contact semi-width a is

$$a(t) = a_0 + a_1 \exp(\iota\omega t), \tag{3}$$

where for plane contact

$$a_0 = \sqrt{\frac{4P_0R}{\pi E^*}}; \quad a_1 = P_1\frac{\partial a}{\partial P} = P_1\sqrt{\frac{R}{P_0\pi E^*}} = \frac{P_1 a_0}{2P_0} \tag{4}$$

and E^* is the composite modulus

$$\frac{1}{E^*} = \frac{(1-\nu_1^2)}{E_1} + \frac{(1-\nu_2^2)}{E_2}. \tag{5}$$

At any given time t, contact extends over $-a(t) < x < a(t)$ and the contact pressure is bounded at the leading edge $x = -a(t)$ and singular at the trailing edge $x = a(t)$. Barber et al. [20] show how to produce a solution that is bounded at the leading edge $x = -a$ and singular at the trailing edge $x = a$, by superposing a series of solutions of a special form. The derivation is somewhat lengthy, and the reader is referred to the paper for details. The results can be rewritten concisely in terms of tangential load and energy dissipation perturbation in full stick, as

$$Q_1 = Q_P P_1 + Q_\Omega \Omega_1; \quad W_1 = W_P P_1 + W_\Omega \Omega_1, \tag{6}$$

where

$$\frac{Q_P(\zeta)}{Q_P^0} = 1 + \frac{\iota\zeta}{2\pi D(\zeta)} I_1\left(\frac{\zeta}{2}\right)\left[1 + \ln\left(\frac{a_0}{2d}\right)\right]; \quad \frac{Q_\Omega(\zeta)}{Q_\Omega^0} = \frac{I_1\left(\zeta/2\right)}{\pi D(\zeta)}, \tag{7}$$

$$\frac{W_P(\zeta)}{V\epsilon_0 Q_P^0} = 1 + \frac{\iota\zeta}{D(\zeta)} J_0\left(\frac{\zeta}{2}\right)\left[1 + \ln\left(\frac{a_0}{2d}\right)\right]; \quad \frac{W_\Omega(\zeta)}{2V\epsilon_0 Q_\Omega^0} = \frac{J_0\left(\zeta/2\right)}{D(\zeta)}, \tag{8}$$

ι is the imaginary unit, ϵ_0 is the mean creep ratio and the function $D(\zeta)$, which has a crucial role in transient effects, is also dependent on the factor $\ln(a_0/2d)$, where d can be interpreted as a measure of the finite dimensions of the contacting body (e.g. the radius of a cylinder),

$$D(\zeta) = J_0\left(\frac{\zeta}{2}\right) - \frac{\iota\zeta}{2\pi} I_1\left(\frac{\zeta}{2}\right)\ln\left(\frac{a_0}{2d}\right) \tag{9}$$

and

$$Q_P^0 = \frac{\epsilon_0}{a_0/R}, \quad Q_\Omega^0 = -\frac{\pi E^* R a_0}{2V} \tag{10}$$

are respectively the values of the functions $Q_P(\zeta)$, $Q_\Omega(\zeta)$ in limit of $\zeta \to 0$, where $\zeta = 2\omega a_0/V$ is a dimensionless frequency and $I_1(p)$ is an integral which can be written in terms of Bessel functions

$$I_1(p) = \int_{-1}^{1} \exp(\iota p s)\sqrt{\frac{1+s}{1-s}}\mathrm{d}s = \pi\left\{J_0(p) + \iota J_1(p)\right\}. \tag{11}$$

In this same limit $\zeta \to 0$, the results of this model coincide with previous results obtained by Ciavarella and Afferrante [8] already perturbing Carter's [21] steady state solution.

2.1. Partial slip 3D solution

The zeroth order coefficient of Carter's solution can be equally simply obtained in the partial slip conditions, not just in full stick. Full stick conditions were assumed only because the full continuum solution under partial slip would involve computation of the energy dissipation in the slip area, by evaluating directly the product of local shear traction, and local microslip. We can however neglect further changes in the ζ dependence of the solution, and hence obtain the coefficients in partial slip. In doing this, we shall also profit to add also the 3D effect, since a full perturbed solution of 3D continuum solution is not viable. In the next paragraph, hence, we shall replace the zeroth order coefficients in the present solution,

with the zeroth order coefficients of the Carter equivalent solution in 3D, with partial slip.

Bhaskar et al. [2] estimate the effect of a true elliptical Hertzian contact by introducing the equivalent of the Carter's solution in 3D which is the case of pure longitudinal creep ratio (we assume no lateral creep) [22], in terms of the tractive ratio $\tau = Q/\mu P$

$$\epsilon = \epsilon_{\max}\left[1-(1-\tau)^{1/3}\right], \tag{12}$$

where Q is the resulting tangential force which is only in the x-direction, and $\epsilon_{\max}$ is given by[2]

$$\epsilon_{\max} = \frac{3\mu}{C_{00}}\left[\frac{16P}{9(1-\nu)^2R_e^2G}\right]^{1/3} \tag{13}$$

with the Kalker's creep coefficient expressed approximately as a function of a/b

$$C_{00} = 2.84 + 1.2\frac{a}{b} \approx 2.84 + 1.2\left(\frac{R}{R_r}\right)^{2/3}, \tag{14}$$

where R is the rolling radius of the wheel, R_r the relative radius of curvature between the wheel and the rail and $R_e = \sqrt{R_r R}$. Now, (12) can be rewritten as

$$Q = \mu P\left(1-\frac{(\epsilon_{\max}-\epsilon)^3}{\epsilon_{\max}^3}\right).$$

It then follows that the dissipation is

$$W = V\epsilon Q = \mu PV\left(1-\frac{\Omega R}{V}\right)\left(1-\frac{(\epsilon_{\max}-(1-(\Omega R/V)))^3}{\epsilon_{\max}^3}\right), \tag{15}$$

where remember that $\epsilon_{\max}$ is a function of P (according to (13)). Hence, by differentiation, we obtain the zeroth order factors, which now depend on tractive ratio τ (or equivalently, the ratio $\epsilon_0/\epsilon_{\max}$), but also on ϵ_0 separately, as as well as friction coefficient

$$Q^0_{P,3D} = \left.\frac{\partial Q}{\partial P}\right|_{P_0,\Omega_0} = \frac{2\mu\epsilon_0}{\epsilon_{\max}}\left(1-\frac{\epsilon_0}{2\epsilon_{\max}}\right), \tag{16}$$

$$Q^0_{\Omega,3D} = \left.\frac{\partial Q}{\partial \Omega}\right|_{P_0,\Omega_0} = -\frac{3\mu RP_0}{V\epsilon_{\max}}\left(1-\frac{\epsilon_0}{\epsilon_{\max}}\right)^2, \tag{17}$$

$$W^0_{P,3D} = \left.\frac{\partial W}{\partial P}\right|_{P_0,\Omega_0} = \frac{2\mu V\epsilon_0^2}{\epsilon_{\max}}\left(1-\frac{\epsilon_0}{2\epsilon_{\max}}\right) = V\epsilon_0 Q^0_{P,3D}, \tag{18}$$

$$W^0_{\Omega,3D} = \left.\frac{\partial W}{\partial \Omega}\right|_{P_0,\Omega_0} = 2\epsilon_0 VQ^0_{\Omega,3D}\left[1+\beta\left(\frac{\epsilon_0}{\epsilon_{\max}}\right)\right], \tag{19}$$

where

$$\beta\left(\frac{\epsilon_0}{\epsilon_{\max}}\right) = \frac{(\epsilon_0/2\epsilon_{\max})(1-(2\epsilon_0/3\epsilon_{\max}))}{(1-(\epsilon_0/\epsilon_{\max}))^2}. \tag{20}$$

In Ciavarella and Barber [8], a Winkler model was used, with Winkler modulus k_q chosen to fit some equations of the Carter solution. However, it resulted that the freedom to choose the Winkler modulus is sufficient to match the steady state solution, but this choice does *not* fit the full perturbed solution not even in the limit $\zeta \to 0$. Specifically, if we fitted the equation for Q_Ω, the other two perturbation coefficients Q_P, W_P could not be matched by a factor 2.

This means the transient effects are more complicated than what a pure Winkler model can predict (as already noticed by Kalker), and indeed similar difficulties have been noticed also by Alonso and Gimenez [23] tuning the Winkler-based code FASTSIM to the exact results of CONTACT. The full perturbation of the continuum CONTACT code has been done by Gross-Thebing [24], and indeed the generalized Kalker coefficients that he defines depend on many factors (geometry of the contact, Poisson's ratio, etc.), and even to get the tangential load (either longitudinal or lateral), the perturbation with respect to many parameters is needed in 3D (longitudinal or lateral creepage, contact area ellipse semi-diameters, peak pressure, etc.). Unfortunately, Gross-Thebing gives very limited results for the energy dissipation which he finds correctly as the integral of density over the slip area.

A possibility that was shown efficient and also based on rigorous arguments in Barber et al. [20], and is here repeated, is changing the ratio $\alpha = (a_0/2d)$, i.e. changing the length scale d, and then assume that all the other relationships remain unchanged from the 2D solution, so that (7) and (8) can be rewritten as

$$\hat{Q}_P(\zeta,\alpha) = \frac{Q_P(\zeta,\alpha)}{Q^0_{P,3D}} = 1 + \frac{\iota\zeta[1+\ln(\alpha)]}{2\pi D(\zeta,\alpha)}I_1\left(\frac{\zeta}{2}\right);$$

$$\hat{Q}_\Omega(\zeta,\alpha) = \frac{Q_\Omega(\zeta,\alpha)}{Q^0_{\Omega,3D}} = \frac{I_1(\zeta/2)}{\pi D(\zeta,\alpha)}, \tag{21}$$

$$\hat{W}_P(\zeta,\alpha) = \frac{W_P(\zeta,\alpha)}{W^0_{P,3D}} = 1 + \frac{\iota\zeta[1+\ln(\alpha)]}{D(\zeta,\alpha)}J_0\left(\frac{\zeta}{2}\right);$$

$$\hat{W}_\Omega(\zeta,\alpha) = \frac{W_\Omega(\zeta,\alpha)}{W^0_{\Omega,3D}} = \frac{J_0(\zeta/2)}{D(\zeta,\alpha)}, \tag{22}$$

where now the zeroth order factors $Q^0_{P,3D}, Q^0_{\Omega,3D}, W^0_{P,3D}, W^0_{\Omega,3D}$ are obtained from the full partial slip 3D Carter solution (Eqs. (16)–(19)), so depend on the ellipticity of the contact, the tractive ratio τ (or equivalently, the ratio $\epsilon_0/\epsilon_{\max}$), but also on ϵ_0 separately, as well as friction coefficient. The dimensionless functions obtained in turn depend on the ellipticity of the contact area via the coefficient α only (although this is the chosen approximation, not a result).

As explained in Barber et al. [20], to choose d, we can best-fit results for the contact ellipticity, Kalker [25] used the matched asymptotic expansion method to expand the general three-dimensional deformation in powers of the small parameter de fining the ratio between the small and large dimensions of the contact region. The first term in this expansion is a two-dimensional solution, but the logarithmic term, corresponding here to the choice of d, is contained in the second term which for more general problems can be obtained as the solution of a line integral equation with a logarithmic kernel. In particular, the tangential compliance of an elliptical contact of semi-axes a and b will be equal to that of a two-dimensional contact of semi-width a with the same force per unit width if the latter is determined using the value

$$d = 2b. \tag{23}$$

When using this approach, an extremely good fit of tangential load results from Gross-Thebing's thesis, par.7.1, i.e., for an ellipticity $b/a_0 = 1.5$, was found, in Barber et al. [20].

3. Global dynamics and limit cases

The dynamic equilibrium of the wheelset, which we simplify now with no stiffness or damping, gives

$$I_w\frac{d\Omega}{dt} = (Q-Q_0)R, \tag{24}$$

[2] We are defining the Kalker coefficients as positive, for simplicity, and hence change the sign of the creep-load relationships as more commonly found in the literature.

where I_w is the inertia of the wheel. Moving to the oscillatory parts therefore, (24) reduces to

$$\iota\omega I_w \Omega_1 = Q_1 R. \tag{25}$$

Substituting Ω_1 from (25) into (6i), and collecting Q_1, and using $\zeta = (2\omega a_0/V)$, we can write the tangential load oscillatory term in the perturbation as a function of the oscillatory term in normal load only

$$Q_1 = \frac{Q_P(\zeta)}{1 - Q_\Omega(\zeta)(R/\iota\omega I_w)} P_1. \tag{26}$$

For dissipation, substituting Ω_1 from (25) into (6ii), we have

$$W_1 = W_P(\zeta)P_1 + W_\Omega(\zeta)\frac{R}{\iota\omega I_w} Q_1 \tag{27}$$

and using (26), (21), (22), we can write it in terms of normal load only

$$W_1 = \left\{ W_P(\zeta,\alpha) + W_\Omega(\zeta,\alpha)\frac{Q_P(\zeta,\alpha)}{(\iota\omega I_w/R) - Q_\Omega(\zeta,\alpha)} \right\} P_1. \tag{28}$$

The present calculation associates dissipation with the position of the wheel, whereas dissipation occur towards the rear of the contact. For this reason the lag of dissipation at a point on the rail is overestimated by about $2\pi a_0/\lambda = \zeta/2$. However, when the tractive ratio is large, dissipation occur nearer the centre of the contact area. For full sliding condition the lag of dissipation at a point on the rail is overestimated by about $\pi a_0/\lambda = \zeta/4$. In between full stick and full sliding we will assume a linear variation with the tractive ratio τ of this correction.

The limit of constant creepage assumed by Grassie and Johnson [7] corresponds to the case where the wheel inertia is very large ($I_w \to \infty$). At the other extreme, the assumption of constant tangential load, as in Grassie and Edwards [26] and Meehan et al. [10], corresponds to the case $I_w \to 0$, where we can notice that assuming additionally $\zeta = 0$, the dissipation function is simplified considerably to nearly the negative of the normal load fluctuation

$$W_1 = -2\mu \frac{\epsilon_0^2}{\epsilon_{\max}} \left(1 - \frac{\epsilon_0}{2\epsilon_{\max}}\right) \left(1 + 2\beta \left(\frac{\epsilon_0}{\epsilon_{\max}}\right)\right) VP_1. \tag{29}$$

This is a remarkably simple result, since now all the locations where the normal load is highest, are automatically the locations of the highest minimum real part of dissipation. This already suggests the assumption of constant tangential load is even too favorable for short pitch corrugation.

4. Example results

The vertical receptance of the rail depends on the particular case. However, the high frequency tail has a single functional form, which depends on a single groups of parameters, and therefore permits to present results of *general validity* in terms of frequency, naturally for this high frequency range. This is extremely convenient, and perhaps corresponds also to the fact that the short pitch corrugation does not depend much on the particular system, as clearly seen in Fig. 1, where, despite railways and intercity systems are included spanning very different technologies (the old BR rails on wooden supports with unwelded rails, the newer continuously welded rails on concrete supports introduced in England by BR after 1966, the Vancouver SkyTrain), the corrugation is seen to have more or less the same features.

This high-frequency tail of rail vertical receptance is described with a simple Euler beam model as in Afferrante and Ciavarella [27]. This simple model show a good agreement with the rail vertical receptance from Bhaskar et al. [2], i.e. a continuous support typical rail for Intercity Track (the paper refers to the Vancouver SkyTrain, but in part II seems to deal with BR track constants), for the frequency of interest for corrugation (greater than about 450 Hz). In other cases, for particularly stiff pads for example, the frequency "crossover" may change, but these would be extreme cases which require separate investigation.

Table 1
Operating parameters.

Young's modulus	$E = 207\,\text{GPa}$
Poisson's ratio	$\nu = 0.3$
Friction coefficient	$\mu = 0.4$
Wheel radius	$R = 0.46\,\text{m}$
Mass of the wheel	$M_w = 350\,\text{kg}$
Inertia of the wheel	$I_w = 27.77\,\text{kg m}^2$
Mass of the rail	$m_{\text{rail}} = 56\,\text{kg/m}$
Inertia of the section area of the rail	$J_{\text{rail}} = 2.35 \times 10^{-5}\,\text{m}^4$
Input ripple, displacement	$\Delta = 50\,\mu\text{m}$

We neglect effect of the pinned–pinned resonance at about 1 kHz, and also the difference between receptance mid-way between sleepers with that at a sleeper. In reality, it would be extremely easy for us to add the lower frequency range, as we have in our database quite a few vertical receptance models. However, choosing the frequency range $f > 450\,\text{Hz}$ permits to have a clean model, which depends only on the asymptotic value of vertical receptance obtained for a simple Euler beam model H_{rail} together with $H_w, 1/k_H$ the concentrated mass receptance of the wheel, and the Hertz linearized contact stiffness, respectively

$$H_{\text{rail}} = \frac{\exp(-\iota 3\pi/4)}{2\sqrt{2}(m_{\text{rail}}^3 E J_{\text{rail}})^{1/4}\omega^{3/2}};$$

$$H_w = -\frac{1}{M_w\omega^2}; \quad k_H = \left[\frac{6G^2 P_0 R_e}{(1-\nu^2)}\right]^{1/3}, \tag{30}$$

where m_{rail} and J_{rail} are the mass and the inertia of the section area of the rail and ω is the circular frequency. From this, the normal load P_1 is evaluated as

$$P_1 = \frac{\Delta}{H_{\text{rail}} + H_w + 1/k_H}, \tag{31}$$

where Δ is the amplitude of the corrugated profile of the rail.

Hence, it is clear that the only parameter in the model here of the rail is $m_{\text{rail}}^3 E J_{\text{rail}}$ and the supporting pad or ballast has no role at this frequency range.

The dissipation function therefore (28), depends in particular on the following parameters, apart from the material and geometric ones:

- inertia of the wheel, I_w;
- steady normal load P_0;
- the tractive ratio $\tau = Q_0/\mu P_0$;
- speed V and wavelength λ (i.e. frequency);
- the shape of contact area, i.e. the ratio of semi-axes b/a_0. This is taken into account in both the zeroth order coefficients via the term $\epsilon_{\max}$ which depends on Kalker's coefficient C_{00}, and in fixing the value of $d = 2b$.

For the inertia, we shall compute

$$I_w = \frac{\psi}{2} M_w R^2,$$

where ψ is a factor ranging in general from 0.5 to 0.8, since the mass of the wheel M_w is concentrated near the centre because of the axle. Nielsen et al. [28] for example report data range from 35 to 125 kg m^2, whereas previous traditional system may have somewhat lower values with mass of the wheel around 350 kg and hence inertia in the range 18–30 kg m^2. For simplicity, we shall consider as

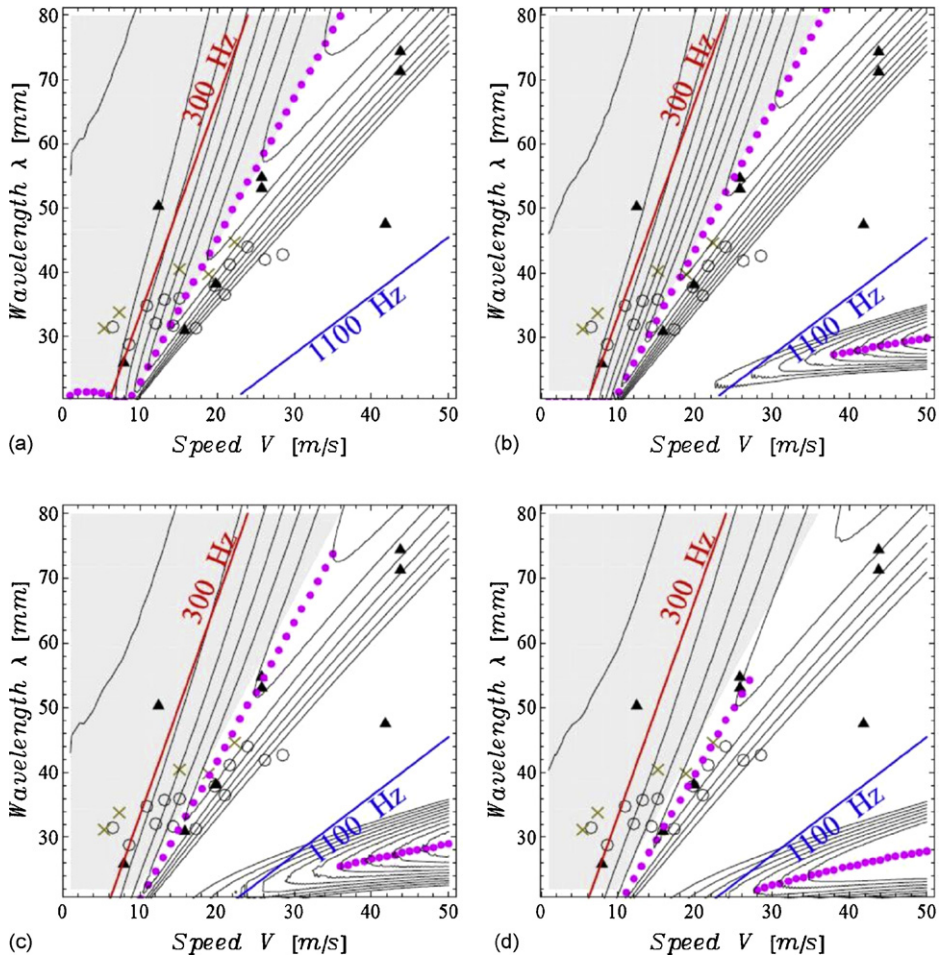

Fig. 3. The expected corrugation wavelength for: (a) $d = 2b = 3a_0$; (b) $d = 2b = 6a_0$; (c) $d = 2b = 9a_0$; (d) $d = 2b = 12a_0$ ($P_0 = 50$ kN; $\tau = 0.1$) (circles BR survey, 1991; triangles Harrison [3]; crosses Vancouver 'SkyTrain', 1992).

a reference case $\psi = 0.75$ and the mass of the wheel 350 kg, with a normal load of 50 kN, as a realistic value for most systems. Reference values are summarized in Table 1.

Fig. 3 shows 10 equally spaced contour levels from zero to the maximum negative real part of dissipation function (28), as a function of speed and wavelength of corrugation. Regular big dots indicate the highest predicted growth for a given speed. Color lines show constant frequency 300, 1100 Hz for reference, also equal to the lines in Fig. 1, and its experimental data points are also included. Since the model for the rail is valid for $f > 450$ Hz, the data should be taken accordingly. The shaded region denotes the zones at frequency $f < 450$ Hz. The four plots of Fig. 3 are obtained for different values of d, and respectively for $d = 2b = 3a_0, 6a_0, 9a_0, 12a_0$. These limits reasonably bracket the range covered by practical variation of d, i.e. of ellipticity of the contact. The contours can be followed by looking at the points of local maxima for any given velocity, in

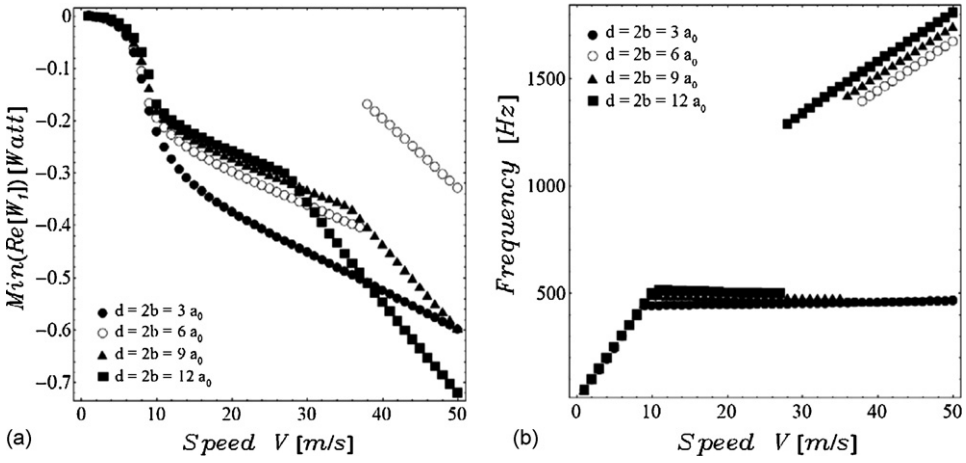

Fig. 4. (a) Variation of the minimum of the real part of W_1 with the speed V for different values of the parameter d ($P_0 = 50$ kN; $\tau = 0.1$); (b) variation of the frequency of corrugation with the speed V for different values of the parameter d ($P_0 = 50$ kN; $\tau = 0.1$).

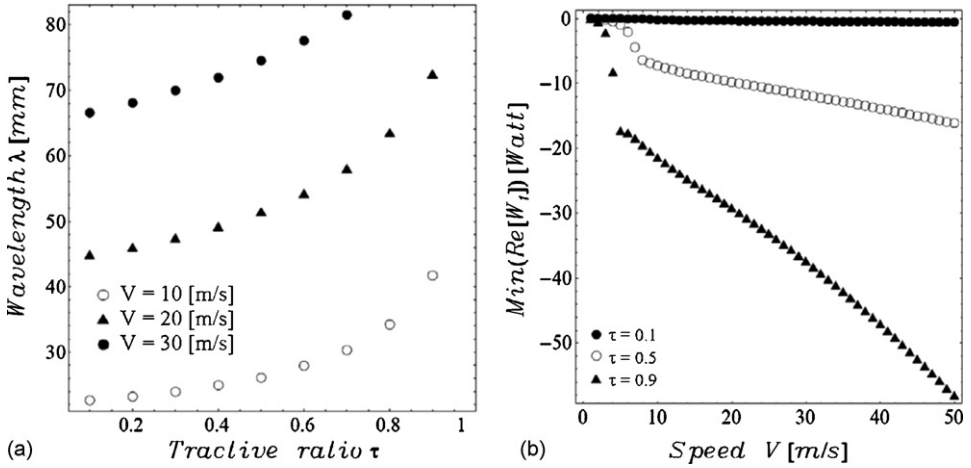

Fig. 5. (a) The expected corrugation wavelength as a function of the tractive ratio τ for different speed V ($P_0 = 50$ kN; $d = 2b = 3a_0$); (b) variation of the minimum of the real part of W_1 with the speed V for different values of the tractive ratio τ ($P_0 = 50$ kN; $d = 2b = 3a_0$).

the range of wavelengths in the figure. Notice two possible regimes of corrugation:

- *at low frequencies (around 500 Hz)* where the wavelength of corrugation is linear with the speed V;
- *at high frequencies* ($>$ 1500 Hz) which compares only for elongated contact where the wavelength of corrugation is almost constant with the speed.

The results of this model in the "nearly circular case" seems surprisingly in general overall agreement with the experimental findings collected in Fig. 1 of Bhaskar et al. [2], despite that considers many different systems and clearly different operating conditions spanning more than a century (old BR data and Harrison's data for British railways, Vancouver SkyTrain).

Fig. 4a and b shows the same results in a different manner, showing the effect of d, i.e. of contact ellipticity is relatively mild, at least with these parameters. In particular, for the same values of the parameter d, we show the variation with the speed V of the minimum of the real part of W_1 and the frequency of corrugation, respectively. Notice the frequency of corrugation is almost constant, not too far from the Winkler results of Ciavarella and Barber [8], and close anyway to 500 Hz.

Fig. 5a shows the effect of the tractive ratio $\tau = Q_0/\mu P_0$ on the expected corrugation wavelength for $d = 2b = 3a_0$. Notice, for fixed speed, the wavelength of corrugation increases with τ (correspondingly the frequency reduces). Fig. 5b shows that the minimum of the real part of W_1 decreases with the speed V, but increases with the tractive ratio τ.

A comparison between constant creepage (large inertia) and constant tangential force (low inertia) is proposed in Fig. 6, to show that the effect of assuming constant creepage, or constant tangential load, is dramatic, and explains why the Grassie and Johnson [7] simplified model could not justify the observed corrugation. In particular, the results seem to suggest that the constant creepage predicts corrugation for very high frequency regimes and with lower growth rates.

Finally, Fig. 7 shows the effect of the steady normal load P_0 on the expected wavelength of corrugation and on the minimum of real part of W_1. Notice the frequency of corrugation increases with the normal load P_0. Also a new regime of corrugation with almost constant wavelength at low speeds appears at high normal loads.

5. Discussion

The present model is limited in many respects:

1. It considers only *longitudinal* mechanisms. Frederick [6] found a factor 20 more likely corrugation in lateral direction for the same creepage ratio, which probably motivated the Berlin group

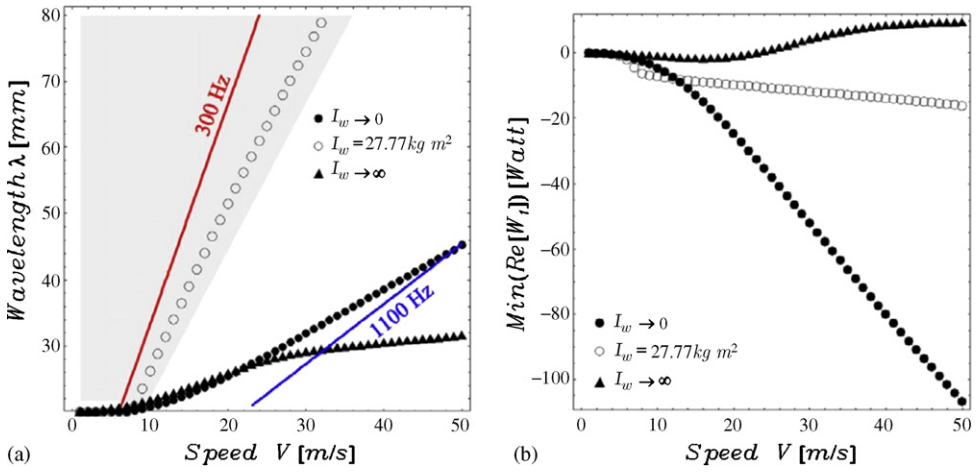

Fig. 6. (a) The expected corrugation wavelength for different inertia: $I_w \to \infty$ (constant creepage), $I_w \to 0$ (constant tangential force), $I_w = 27.77$ kg m^2 ($P_0 = 50$ kN; $d = 2b = 3a_0$; $\tau = 0.5$); (b) variation of the minimum of the real part of W_1 with the speed V for different inertia ($P_0 = 50$ kN; $d = 2b = 3a_0$; $\tau = 0.5$).

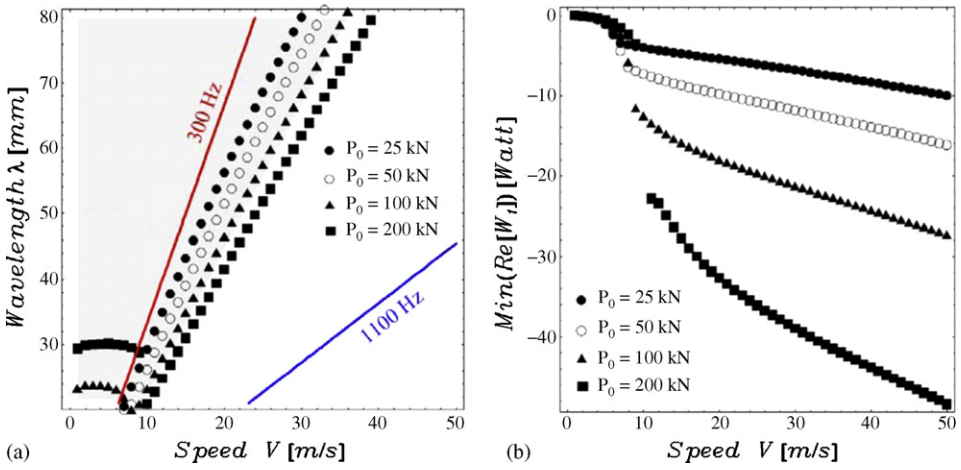

Fig. 7. (a) The expected corrugation wavelength for different steady normal load P_0 ($d = 2b = 3a_0$; $\tau = 0.5$); (b) variation of the minimum of the real part of W_1 with the speed V for different P_0 ($d = 2b = 3a_0$; $\tau = 0.5$).

to look only at lateral creepage. However, the same Frederick, in the discussion of the Hempelmann and Knothe [14] paper, suggests to include longitudinal creepage, as more likely to be much higher—up to 10 times higher than lateral one. Hence, since corrugation grows with the square of creepage, here we have a factor 100 in favor of the longitudinal mechanisms. It is clear that in conditions with significant lateral creepage, this should be further examined, and the present paper does not give enough details to make the comparison.

2. It neglects possible coupling between low-frequency and high-frequency, which however has often been found to be indeed negligible [2]. In general, the corrugation phenomena can be justified if one takes an initial spectrum of roughness, and looks at the transient amplification. Since the initial spectrum contains various frequencies and in general more frequency content in the longer wavelengths, the appearance of corrugation in the short term may be different from the long term one, where one expects that nonlinearity would lead to a limit cycle. Normally, it is considered that for example, when amplitude of corrugation in the short-pitch range reaches about 80 μm there is loss of contact, but by then the noise is so large that most system maintenance strategies would have had to recur to grinding—indeed most railways grind at amplitudes of about 50 μm.
3. It does not consider discrete supports, although we shall make some estimates in the next paragraph using the typical approximate treatment considering local values of stiffness. What we have done so far is valid for a continuous support model, or as another approximation to the problem, considering a smoothed out version of a discrete support model. In fact, many resonances are neglected in models under the assumption that they are "narrow". This may be the case of the pinned–pinned resonance too, as in Bhaskar et al. [2]. On the contrary, the approximation of the local approach neglects parametric resonance effects, which we have explored only with a simplified model [29].
4. It does not consider interaction between wheels in waves reflecting from one end to the other, and the many other possible mechanisms for corrugation or interactions.

A general problem in this area was the unfortunate circumstance that there was never much discussion and comparison of models, many problems appear "specific" and prone to various interpretation. A good review of the corrugation problems in the railways is in the Hempelmann thesis (1996). Interesting the case of BR, who had long collected data but did admit serious corrugation problems only in the 1970s after the 1966 introduction of the concrete sleepers and continuously welded rails. Surprisingly however, only on the West Coast Main Line had problems, and not on the East one (probably because of different re-railing with lesser conicity), and also the corrugation stopped at the Scottish border where Acid Bessemer steel was replaced by Open Heart steel (a difference that is

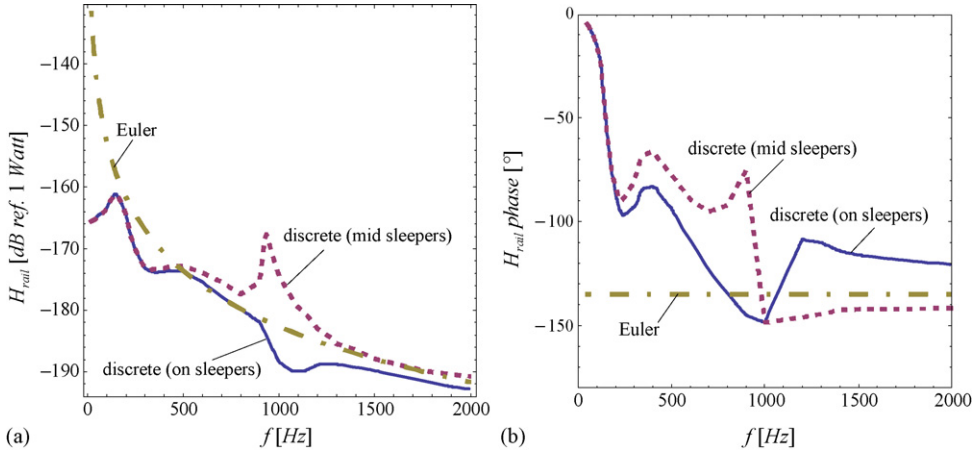

Fig. 8. Vertical receptance for a rail under discrete support taken from Grassie et al. [19] shown in their Fig. 7 corresponding to concrete pads on a typical BR rail used after the 1970s (pad stiffness 280 MN/m, pad mass 110 kg, rail mass 56 kg/m). The receptance above the sleepers, and midsleepers, is show schematically together with the continuous approximation in the asymptotic high frequency tail for Euler beam.

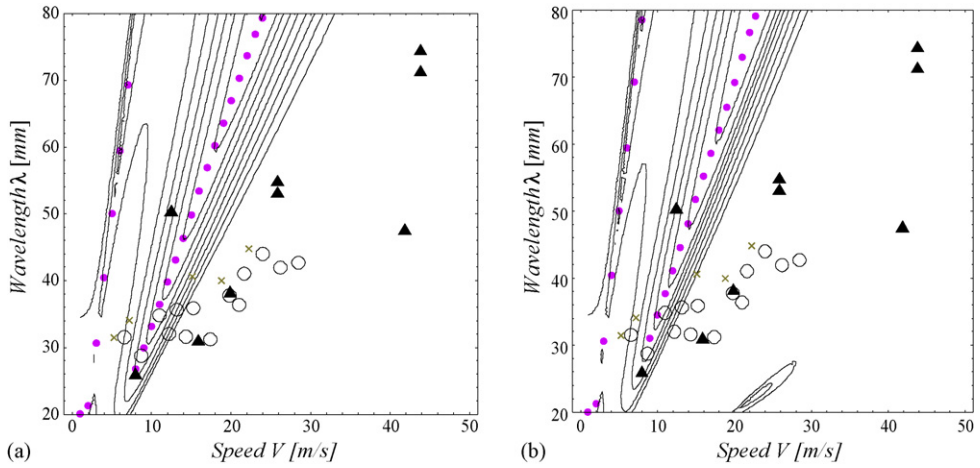

Fig. 9. The expected corrugation wavelength for discrete supports (model of Fig. 8) with excitation force (a) on sleepers; (b) between sleepers ($d = 2b = 3a_0$; $\tau = 0.5$; $P_0 = 50$ kN).

still mostly unexplained!). Later, BR stopped research and remained mostly monitoring. The Chinese railways report corrugation when track irregularity disturb the hunting motion of the vehicle. USA, Canada and Australia mostly have long-pitch corrugation, while metro systems tend to have problems in curves. German railways (DB) have operated various test sites and found also that Thomas steel was more likely to corrugate than Martins steel, and corrugation was seen to depend on rail inclination. The Dutch seem to have been between the first to use the idea of "preventative grinding" on rails within the first 6 months after their pose because "for reasons

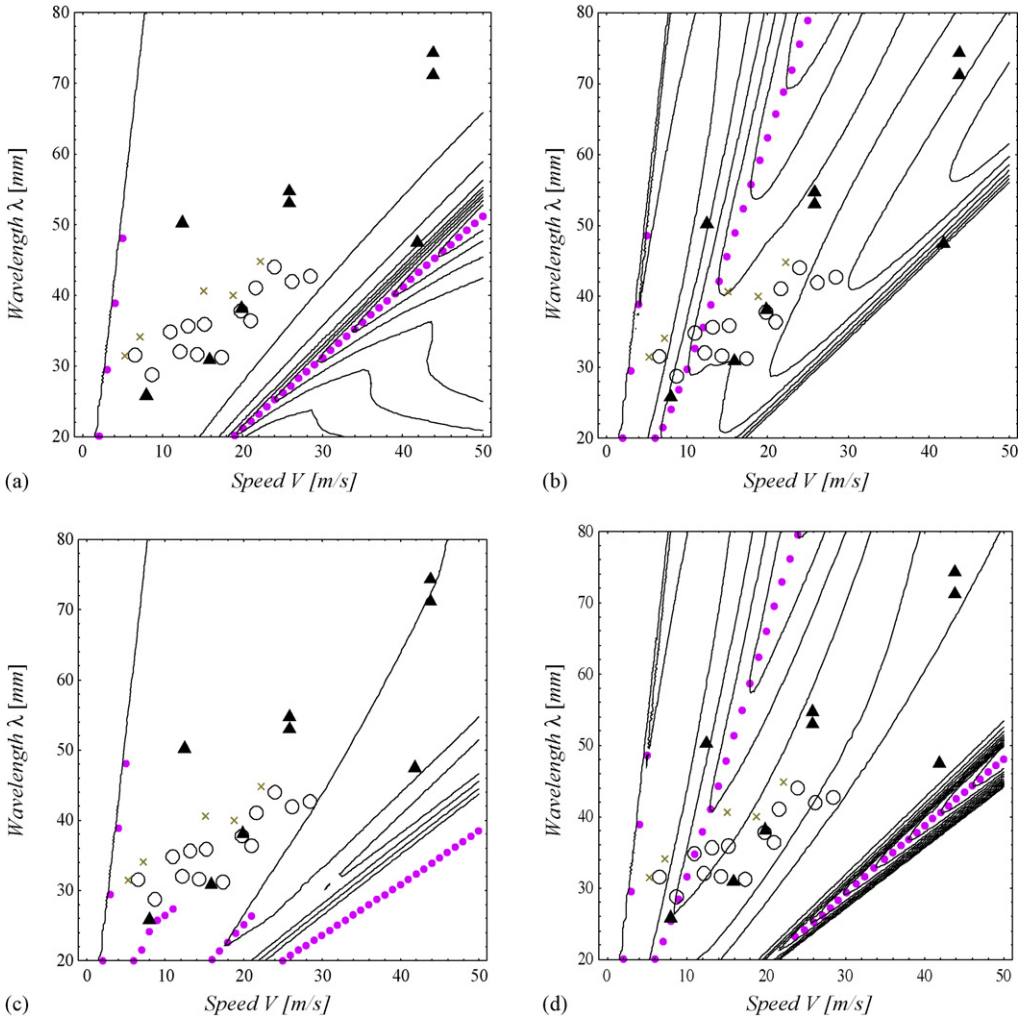

Fig. 10. The expected corrugation wavelength for a model with discrete supports but transient effect removed ("steady model"): (a) $I_w \to 0$ with excitation force on sleepers; (b) $I_w = 27.78$ kg m^2 with excitation force on sleepers; (c) $I_w \to 0$ with excitation force between sleepers; (d) $I_w = 27.78$ kg m^2 and excitation force between sleepers ($d = 2b = 3a_0$; $\tau = 0.5$; $P_0 = 50$ kN).

unknown" rail corrugation started only rarely on such ground rails before they had seen significant traffic [30]. Similar forms of "preventive grinding" or "regular grinding" is also the routine solution for many railways (French never have admitted much corrugation problems probably because of a very serious such maintenance program), and while steels are harder and harder and wear in principle is reduced, regular grinding is nowadays conducted also as a means to reduce cracks anyway [31] but this becomes then a matter hard to judge scientifically also because of lack of data and the presence obvious commercial, managerial and political interests.

To give an idea of the complexity of the problem which induces at time trivial errors, and on the other hand of the unfortunate lack of serious collaboration between industries and universities in the field, in the end of the 1990s, ERRI (European Railways Research Institute, which did not survive very long) sponsored some research in order to make a comparison of predictive capabilities of the various models (Frederick' BR one, Berlin ones, Cambridge ones). This is hardly mentioned in the literature (perhaps for the prohibitive cost of these reports) but it is unfortunate, since they are extremely interesting and elucidating.

In the report D185/RP1 [32], various interesting facts are worth reporting:

(a) There was general agreement between the corrugation growth rate prediction (surprisingly to us since Berlin used a full 3D contact solution, while BR used a simplified method) at least up to 1200 Hz, then considerable differences at 1500 Hz.
(b) There was a difference in the vertical receptance by a factor 10 or 20, which is certainly not a good start for any modelling!

In another such useful report [33], not only more models are compared (Hempelmann's, Frederick in the extended 3D contact version of 1991, Bhaskar's model from Cambridge, a large creepage model from Clark at BR, and the Tassilly model by RATP and Vibratec), but an attempt is made to compare to experimental measurements on test sites. The 1993 findings were repeated, probably the 1500 Hz regime difference was associated to difference in calculating wear in the contact area. The experimental validation was extremely confusing, and even giving to the models the roughness input at the starting conditions, there was only vague qualitative agreement. But the most striking finding was that in the test site there was development of the 20 mm roughness that everyone had considered to be "suppressed by contact filter"!

6. Final remarks on pinned–pinned resonance

Since our model does not consider discrete supports, our claim that pinned–pinned resonance may have been overestimated as a explanation for short-pitch corrugation, remains somehow weak. Hence, in this paragraph we attempt to address the question more precisely, although limiting attention to the longitudinal mechanisms.

First, we shall consider a discrete support receptance for the rail taken from the Literature, in particular, that due to Grassie et al. [19] shown in their Fig. 7 corresponding to concrete pads on a typical BR rail used after the 1970s (pad stiffness 280 MN/m, pad mass 110 kg, rail mass 56 kg/m). The receptance above the sleepers, and midsleepers, is show schematically in Fig. 8, together with the continuous approximation in the asymptotic high frequency tail for Euler beam.

Fig. 9 shows the energy dissipation function using the receptance above sleepers and mid-sleepers, locally. Clearly, there is no corrugation growth predicted at the pinned–pinned resonance, whereas corrugation is predicted to growth at about 300 Hz, slightly differently from the results of the continuous model. Notice that this is equally true above or mid-sleepers, naturally because at that frequency the two receptances are identical. On the contrary, the predicted corrugation growth was found at lower frequency than in the model with continuous support, due to a more marked anti-resonance at about 300 Hz in that model.

In connection to the results of Xie and Iwnicki [12], we tried to make the same estimates using a model with the transient effects removed ("steady", in their terminology), and instead we find possible corrugation between sleepers (Fig. 9). However, when using their assumption of constant tangential load (zero inertia of the wheel) we did find large differences but not between steady and non-steady model (Fig. 10), and anyway not suggesting absence of corrugation growth. Their results therefore appear in contrast to our findings.

We are not in a position to completely clarify the source of the rather contrasting results, but according to the experiments just presented, or similar recent investigations (see Afferrante and Ciavarella [27] where non-steady effects are neglected, in comparison with Barber and Ciavarella [8], where non-steady effect are included), we find that the critical assumption concerns the tangential dynamics of the system, more than steady vs. non-steady. When authors assume constant creepage, like Grassie and Johnson [7], our investigations suggest corrugation suppression instead of corrugation growth, explaining the negative conclusions of Grassie and Johnson [7]. Constant tangential load seems in our findings not to lead to corrugation suppression, but actually enhancement of the growth. In particular, the frequency corresponding to the highest growth of corrugation is close to the pinned–pinned resonance, despite we do not include that resonance in the model.

On reflection, our findings in longitudinal direction correspond and confirm previous findings by Frederick [6] where the phase appears not appropriate for corrugation. Hence, the lateral direction mechanism, which Frederick reported of possible growth at the pinned–pinned resonance, requires some additional effort and investigation.

7. Conclusions

Despite the large literature review on the problem, different models in the literature make very different assumptions, and hardly make estimates over the entire frequency range, so that a full comparison over the "dominant" mechanism of corrugation is still very difficult to make, and is necessarily system-specific. In this paper, far from giving a final answer to this problem, we have reviewed some results, and suggested a new mechanism (in pure longitudinal direction) as a possible alternative for the corrugation data which fall outside the pinned–pinned resonance range. This is particularly appropriate and perhaps the only explanation when the support is indeed continuous and not discrete, and where corrugation has also been observed outside the resonant frequencies, possibly with indication that longitudinal creepage is the most important mechanism. In particular, our main interest is in the frequency range higher than about 450 Hz, where we can use the asymptotic tail of the Euler beam solution for the rail receptance, which is independent on the details of the pad and the supports.

From the contact mechanics point of view, we have suggested an approximate but simple solution generalizing the 2*d* continuum full stick problem found in Barber et al. [20], for elliptical contact and partial slip. Contrary to the models assuming constant creepage [7,2], the results show a possible regime of corrugation, as they suggest possible growth of corrugation.

As final remarks on pinned–pinned resonance, we made some experiments using a discretely supported model, corresponding to a typical BR rail with concrete pads. We did not find evidence of

possible corrugation growth at the frequency of pinned–pinned resonance, neither above pads, or above pads, in longitudinal direction. On the contrary, the predicted corrugation growth was found at lower frequency than in the model with continuous support, due to a more marked effect of the anti-resonance at about 300 Hz in that model.

Anyway, given the still limited capabilities of the models, and the effects which we have omitted (lateral direction mechanisms, for example), we prefer to maintain a prudent agnostic view over which mechanism is dominant, as this is likely anyway to be system-specific. The comparison between lateral mechanisms and longitudinal inevitably depends on the absolute value of lateral and longitudinal creepage, the latter generally being often much larger than the former, and this difference is likely to be enhanced as corrugation growth factor, since this is proportional to the square of creepage ratio.

We prefer to indicate the regime found here as very persistent, since it would be present in most systems due to the high frequency tail of the rail receptance, which depends only on the rail itself, and not the details of the supports.

References

[1] S.L. Grassie, J. Kalousek, Rail corrugation: characteristics, causes and treatments, J. Rail Rapid Transit, Proc. Inst. Mech. Eng. 207F (1993) 57–68.
[2] A. Bhaskar, K.L. Johnson, G.D. Wood, J. Woodhouse, Wheel-rail dynamics with closely conformal contact. Part 1. Dynamic modelling and stability analysis, IMechE Proc. Inst. Mech. Eng. 211 (Part F) (1997) 11–26.
[3] D. Harrison, Corrugation of railways, PhD Thesis, Cambridge University, UK, 1979.
[4] R.M. Carson, K.L. Johnson, Surface corrugations spontaneously generated in a rolling contact disc machine, Wear 17 (1971) 59.
[5] K.L. Johnson, G.G. Gray, Development of corrugations on surfaces in rolling contact, Proc. Inst. Mech. Eng. Lond. 189 (1975) 45–58.
[6] C.O. Frederick, A rail corrugation theory, in: Proceedings of the 2nd International Conference on Contact Mechanics of Rail-Wheel Systems, University of Waterloo Press, University of Rhode Island, 1986, pp. 181–211.
[7] S.L. Grassie, K.L. Johnson, Periodic microslip between a rolling wheel and a corrugated rail, Wear 101 (1985) 291–305.
[8] M. Ciavarella, J.R. Barber, Influence of longitudinal creepage and wheel inertia onshort-pitch corrugation: a resonance-free mechanism to explain the roaring rail phenomenon, Proc. IMechE, Part J: J. Eng. Tribol. 222 (2008) 1–11.
[9] S.L. Grassie, Rail corrugation: advances in measurement, understanding and treatment, Wear 258 (7–8) (2005) 1224–1234.
[10] P.A. Meehan, W.J.T. Daniel, T. Campey, Prediction of the growth of wear-type rail corrugation, Wear 258 (7–8) (2005) 1001–1013.
[11] T.X. Wu, D.J. Thompson, An investigation into rail corrugation due to micro-slip under multiple wheel/rail interactions, Wear 258 (2005) 1115–1125.
[12] G. Xie, S.D. Iwnicki, Simulation of roughness growth on rails—results from a 2D non-Hertzian, non-steady contact model, Vehicle Syst. Dyn. 46 (1–2) (2008) 117–128.
[13] K. Knothe, A. Groß-Thebing, Short wavelength rail corrugation and non-steady-state contact mechanics, Vehicle Syst. Dyn. 46 (1–2) (2008) 49–70.
[14] K. Hempelmann, K. Knothe, An extended linear model for the prediction of short pitch corrugation, Wear 191 (1996) 161–169.
[15] K. Hempelmann, Short Pitch Corrugation on Railway Rails—A Linear Model for Prediction, VDI Fortschritt-Berichte, Reihe 12, No. 231, Dusseldort, 1994.
[16] T.X. Wu, D.J. Thompson, On the rolling noise generation due to wheel/track parametric excitation, J. Sound Vib. 293 (3–5) (2006) 566–574.
[17] X. Sheng, D.J. Thompson, C.J.C. Jones, G. Xie, S.D. Iwnicki, P. Allen, S.S. Hsu, Simulations of roughness initiation and growth on railway rails, J. Sound Vib. 293 (3–5) (2006) 819–829.
[18] T.X. Wu, D.J. Thompson, On the parametric excitation of the wheel/track system, J. Sound Vib. 278 (4–5) (2004) 725–747.
[19] S.L. Grassie, R.W. Gregory, D. Harrison, K.L. Johnson, The dynamic response of railways track to high frequency vertical excitation, Int. J. Mech. Sci. 24 (1982) 77–90.
[20] J.R. Barber, M. Ciavarella, L. Afferrante, A. Sackfield, Effect of small harmonic oscillations during the steady rolling of a cylinder on a plane, Int. J. Mech. Sci. 50 (2008) 1344–1353.
[21] F.W. Carter, On the action of a locomotive driving wheel, Proc. Roy. Soc. Lond. Ser. A (1926) 151–157.
[22] P.J. Vermeulen, K.L. Johnson, Contact of non-spherical bodies transmitting tangential forces, J. Appl. Mech. 31 (1964) 338–340.
[23] A. Alonso, J.G. Giménez, Non-steady state modelling of wheel-rail contact problem for the dynamic simulation of railway wheels, Vehicle Syst. Dyn. 45 (2007) 1–18.
[24] A. Gross-Thebing, A lineare Modellierung des instationaren Rollkontaktes von Rad und Schiene, VDI Fortschritt-Berichte, Reihe 12, No. 199, Dusseldort, 1993.
[25] J.J. Kalker, On elastic line contact, ASME J. Appl. Mech. 39 (1972) 1125–1132.
[26] S.L. Grassie, J.W. Edwards, Development of corrugation as a result of varying normal load, in: Proceedings of the 7th Interenational Conference on Contact Mechanics and Wear of Rail/Wheel Systems (CM2006), Brisbane, Australia, September 24–26, 2006.
[27] L. Afferrante, M. Ciavarella, On corrugation models and the "roaring rails" enigma: a simple analytical contact mechanics model based on a perturbation of Carter's solution, J. Mech. Mater. Struct., in press, http://pjm.math.berkeley.edu/scripts/coming.php?jpath=jomms.
[28] J.C.O. Nielsen, A. Ekberg, R. Lundén, Influence of short-pitch wheel/rail corrugation on rolling contact fatigue of railway wheels, Proc. Inst. Mech. Eng., Part F: J. Rail Rapid Transit 219 (3) (2005) 177–187.
[29] N.P. Hoffmann, M. Ciavarella, U. Stolz, C. Weiß, The effect of long-wavelength stiffness variation on wear pattern generation, J. Sound Vibration, submitted for publication. Available online 1 January 2009 on www.sciencedirect.com.
[30] R.A. Van der Bosch, Les strafegies de meulage des chemin de fer neerlandais, Revue Generale des Chemins de Fer, nov. (2002) 40–43.
[31] S.L. Grassie, P. Baker, Routine maintenance extends rail life and offers long-term savings, Railway Gazette Int. (February 2000) 88–90.
[32] ERRI D185/RP1, Reduction of rail corrugation, Rail corrugation models—comparison of results obtained using the Berlin Technical University and British rail methods, 1993.
[33] ERRI-D185WP2, Theoretical modelling of rail corrugations and validation by measurement, 1997.